Journal of Power Sources 196 (2011) 10032–10037

Contents lists available at ScienceDirect

Journal of Power Sources

journal homepage: www.elsevier.com/locate/jpowsour

Improvement of corrosion resistance and electrical conductivity of 304 stainless steel using close field unbalanced magnetron sputtered carbon film

Weihong Jin[a], Kai Feng[a], Zhuguo Li[a,*], Xun Cai[a], Lei Yu[b], Danhua Zhou[b]

[a] Shanghai Key laboratory of Materials Laser Processing and Modification, School of Materials Science and Engineering, Shanghai Jiao Tong University, Shanghai 200240, PR China
[b] Zhejiang Huijin-Teer Coatings Co., Ltd., Lin'an 311305, PR China

ARTICLE INFO

Article history:
Received 5 August 2011
Accepted 9 August 2011
Available online 16 August 2011

Keywords:
Bipolar plates
Stainless steel
Carbon film
Corrosion resistance
Interfacial contact resistance

ABSTRACT

Carbon film has been deposited on 304 stainless steel (SS304) using close field unbalanced magnetron sputter ion plating (CFUBMSIP) to improve the corrosion resistance and electrical conductivity of SS304 acting as bipolar plates for proton exchange membrane fuel cells (PEMFCs). The corrosion resistance, interfacial contact resistance (ICR), surface morphology and contact angle with water of the bare and carbon-coated SS304 are investigated. The carbon-coated SS304 shows good corrosion resistance in the simulated cathode and anode PEMFC environment. The ICR between the carbon-coated SS304 and the carbon paper is 8.28–2.59 $m\Omega\,cm^2$ under compaction forces between 75 and 360 $N\,cm^{-2}$. The contact angle of the carbon-coated SS304 with water is 88.6°, which is beneficial to water management in the fuel cell stack. These results indicate that the carbon-coated SS304 exhibits high corrosion resistance, low ICR and hydrophobicity and is a promising candidate for bipolar plates.

1. Introduction

The proton exchange membrane fuel cell (PEMFC) has been considered to be important for industries in the energy realm and has attracted considerable interest from the research community because of its promise as a driving force for electric vehicles. Bipolar plates are essential in PEMFCs [1] and account for a large percent of the mass and cost in the PEMFC stack [2,3]. They conduct current between cells, separate reactant gases, i.e., hydrogen and oxygen (or air), and facilitate water and thermal management through the cell [4,5]. Therefore, bipolar plates possess high electric conductivity, good corrosion resistance, high mechanical strength, high gas impermeability, light weight and low cost [3]. Because durability and cost are two main challenges hindering this fuel technology from penetrating the energy market, it is critical to improve the performance of bipolar plates to achieve the commercial use of PEMFC.

Stainless steels are considered to be good candidates for bipolar plate materials in PEMFC due to their low cost, high strength, and ease of fabrication into thin sheets. However, the fatal flaw of stainless steel is its tendency to corrode in the harsh acidic and humid environment inside the PEMFC without forming passive layers [4]. The passive film formed under the cathode on the surface protects the metal from progressive corrosion but also decreases the surface electrical conductivity [6], which leads to the dissipation of some electric energy into heat and reduces the overall efficiency of the fuel cell stack. Meanwhile, the metal ions produced by corrosion contaminate the membrane exchange assembly, which results in the degradation of the performance of the PEMFC stack [7–10].

Improved corrosion resistance and electrical conductivity appear to be difficult to achieve simultaneously for stainless steels, but it is possible to achieve both by coating technology [11–13], and surface modification is an important method to improve the performance of stainless steel bipolar plates. Close field unbalanced magnetron sputter ion plating (CFUBMSIP) [14] is an advanced and well-established technology that generates coatings that are dense with few defects, that firmly adhere to the substrate and that have very low inner stress. Carbon film with a high sp^2 percentage is one coating candidate that can be used for stainless steel bipolar plates due to its high electrical conductivity, chemical inertness and hydrophobicity [15–17]. Researchers have performed many studies on 316L stainless steel (SS316L) [18–21], but few studies have focused on improving the corrosion resistance and electrical conductivity of 304 stainless steel (SS304). SS304 costs less than SS316L and is a very promising material for bipolar plates. In this paper, to combine the merits of both SS304 and carbon, carbon film is coated on SS304 by CFUBMSIP. The carbon film thickness, surface morphology, corrosion resistance, electrical conductivity and contact angle with water are investigated.

* Corresponding author. Tel.: +86 21 34202837; fax: +86 21 34203024.
E-mail address: lizg@sjtu.edu.cn (Z. Li).

0378-7753/$ – see front matter.
doi:10.1016/j.jpowsour.2011.08.050

2. Experimental details

The SS304 samples were used as substrates for the bipolar plates. Both sides of the samples were polished with No. 2000 SiC waterproof abrasive papers, cleaned with acetone in an ultrasonic cleaner for 15 min, and then dried. The carbon film was deposited on the substrates by a CFUMSIP system consisting of two 99.99% pure graphite targets and two targets of 99.99% Cr. The SS304 sample was immersed in the plasma atmosphere during deposition. Before deposition, the substrates were sputtered by plasma at a −500 V bias voltage to clean the substrate surfaces and obtain an active surface to improve the adhesion strength between the substrates and the film. To achieve a uniform film, the substrates were rotated at 2.5 r min^{-1}. As a transition layer, chromium carbide was first deposited on the substrates with all four targets working to enhance adhesion. Then, the pure carbon coating was deposited using the two carbon targets. To achieve high-performance carbon film, this experiment improved the deposition parameters compared to those in the previous work [22].

The thickness of the carbon film on the SS304 was measured using a similar method to that reported by Zhang [23] with a crater machine (BC-2, Teer Coatings, Ltd.). The test specimen, carbon-coated SS304, was put on the inclined specimen stage of the crater machine and then experienced friction from the steel ball during which silicon carbide paste was smeared on the test specimen. Then, a spherical crater appeared on the surface of the specimen. After the removal of the silicon carbide paste on the surface of the carbon coated SS304, professional computer software was used to accurately calculate the thickness of each layer of carbon film on the SS304. The surface morphology of the carbon-coated SS304 before and after the potentiostatic tests was observed by ultra high resolution thermal FE SEM (JSM-7600F, JEOL). Because hydrophobic bipolar plates can effectively prevent water flooding in the PEMFC stack, the contact angle of the carbon-coated SS304 with water was measured with a video-based contact angle measuring device (OCA 20, Dataphysics).

The electrochemical measurements were conducted on the advanced electrochemical system (PARSTAT 2273, Princeton Applied Research, a subsidiary of AMETEK, Inc) using a three-electrode cell. The three-electrode cell was composed of the sample as the working electrode, a graphite rod as the counter electrode and a saturated calomel electrode (SCE) as the reference electrode. Unless otherwise stated, the potential is referenced against the saturated calomel electrode. To simulate the operation conditions of PEMFC, all of the electrochemical experiments were conducted in 0.5 M H_2SO_4 + 2 ppm HF at 80 °C. Because bipolar plates in PEMFC are exposed to air/oxygen on one side and to hydrogen gas on the other, the solution was bubbled either with pressured air (to simulate the PEMFC cathode environment) or with hydrogen gas (to simulate the PEMFC anode environment) during the measurements reported by Fukutsuka et al. [15], Wang and Northwood [24] and Choi et al. [25]. To ensure the electrochemical stability of the system, the open circuit potential (OCP) was tested for 30 min before the potentiodynamic tests. To clarify the electrochemical behaviour, the potentiodynamic curve was tested at a potential scanning rate of 1 mV s^{-1}. Because the bipolar plates corrode at the operating voltage (0.6 V and −0.1 V in the simulated cathode and anode environments, respectively), the potentiostatic tests were conducted for 4 h to investigate the stability of the carbon film. During the potentiostatic tests, the cathode condition was applied with 0.6 V and bubbling with air, and the anode condition was applied with −0.1 V and bubbling with hydrogen.

The interfacial contact resistance between the bipolar plate and the gas diffusion layer is an important property of bipolar plates for PEMFC and significantly affects the power output of the fuel cell stack. Therefore, the interfacial contact resistance between the carbon-coated SS304 and conductive carbon paper (Toray TGP-H-060) was evaluated by a method similar to that reported by Wang et al. [26]. A schematic illustration of the ICR measurement is shown in Fig. 1. In this measurement, two pieces of carbon papers were sandwiched between the coated sample and two copper plates. An outside force was applied on the two insulators above and below the upper and lower copper plates, respectively. The two copper plates were connected to an ohmmeter to measure the total resistance of the assembly. One piece of carbon paper was sandwiched between two copper plates, and the ICR between the copper plate and the carbon paper was also tested to calibrate the ICR between the carbon film and the carbon paper.

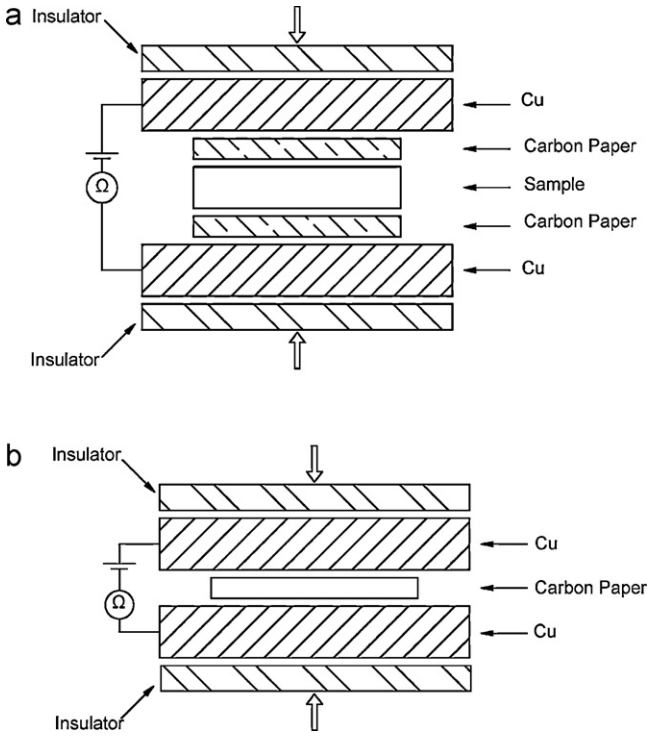

Fig. 1. Schematic illustration of the setup used to measure interfacial contact resistance.

3. Results and discussion

3.1. Carbon film characterisations

The thickness measurement of the carbon film on SS304 is shown in Fig. 2. It can be seen that the total thickness of the carbon film is 3.09 μm, including a 1.06 μm translation layer and 2.03 μm pure carbon film. The translation layer is deposited because of its good adhesion to both the substrate and the pure carbon film. Meanwhile, the pure carbon film can protect the substrate against corrosion.

Fig. 3 shows a SEM image of a surface micrograph of the carbon film on SS304. The picture shows a flat, uniform, homogeneous film. In our range of observation, no obvious pinhole is observed, and the carbon film is dense. Thus, this carbon film significantly improves the corrosion resistance of the SS304 bipolar plates because in the CFUBMSIP process, there is a high ion current density surrounding the substrates and intense ion bombardment on the growing film that are beneficial for dense deposition with few defects and well-adhered films.

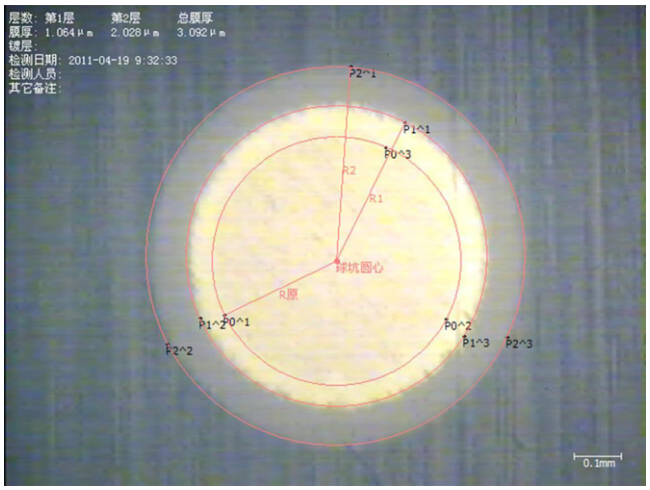

Fig. 2. Thickness measurement of the carbon film on SS304.

3.2. Electrochemical measurements

The open circuit potential with respect to time is tested in 0.5 M H_2SO_4 + 2 ppm HF at 80 °C before the potentiodynamic test, and the results are shown in Fig. 4. The electrochemical test results of SS316L are also added into the graphs as a control. It can be seen that the uncoated and carbon-coated SS304 quickly reach a constant value in both the simulated cathode and anode environments, which indicates that the system reaches a stable state. The OCP of the uncoated SS304 and SS316L stabilise at −356 mV and −286 mV in the simulated cathode environment and stabilise at −357 mV and −307 mV in the simulated anode environment. Compared to the uncoated SS304, the carbon-coated SS304 has a more stable OCP, which increases to 206 mV and 214 mV in the simulated cathode and anode environments, respectively. The carbon-coated SS304 exhibits higher OCP in both the simulated cathode and anode environments and is approximately 560 mV more positive than that of the uncoated SS304 and approximately 500 mV more positive than that of the uncoated SS316L. Therefore, the carbon-coated SS304 has a much lower corrosion tendency and better corrosion resistance than the uncoated SS304 and SS316L in the simulated PEMFC environment.

Fig. 5 shows the potentiodynamic curves of the bare SS304 and SS316L and the carbon-coated SS304 in the simulated cathode and anode PEMFC environments. Both the bare SS304 and SS316L have a stable passive region in the simulated cathode and anode environments. The critical passive current density and passive current density of the bare SS316L are lower than those of the bare SS304, which indicates that SS316L easily reaches the stable state and has better stability than SS304 in the simulated PEMFC environment. As shown in Fig. 5(a), the corrosion current density of the bare SS304 and SS316L are 38.01 μA cm^{-2} and 11.26 μA cm^{-2} at 0.6 V (the cathodic operation potential) in the simulated cathode environment, respectively. Both the bare SS304 and SS316L are in the passive state at the cathodic operation potential. The carbon-coated SS304 does not have an obvious passive state in the test potential region, but the corrosion current density of the carbon-coated SS304 significantly decreases to 2.10 μA cm^{-2} at the cathodic operation potential, which is one order of magnitude lower than that of the bare SS304 and SS316L. The smaller anode corrosion current density often corresponds to a low corrosion rate and high corrosion resistance.

Fig. 5(b) shows that the corrosion current density of the bare SS304 and SS316L are 92.42 μA cm^{-2} and 25.79 μA cm^{-2} at −0.1 V (the anodic operation potential) in the simulated anode environment, respectively. However, in the simulated anode environment, the corrosion potential of the carbon coated SS304 moves to the right to approximately 0.2 V, which is more positive than the anodic operation potential of −0.1 V. Thus, the carbon film is in the cathodic state and can protect SS304 against corrosion in the simulated anode environment.

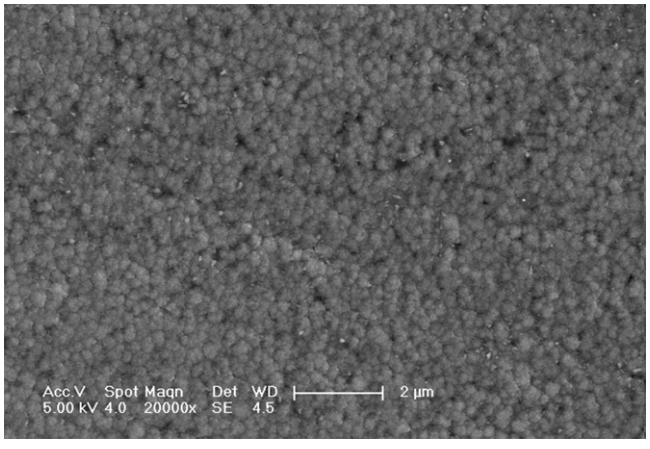

Fig. 3. SEM image of the surface micrograph of the carbon film on SS304.

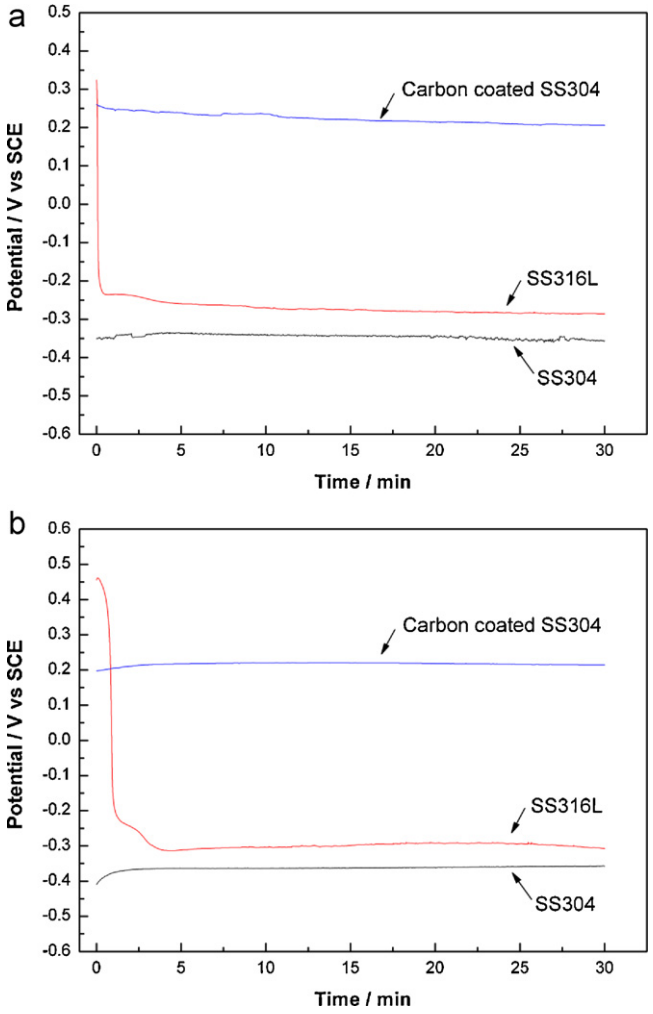

Fig. 4. Open circuit potential of SS304, SS316L and the carbon-coated SS304 in 0.5 M H_2SO_4 + 2 ppm F^- solution at 80 °C: (a) bubbled with air and (b) bubbled with hydrogen.

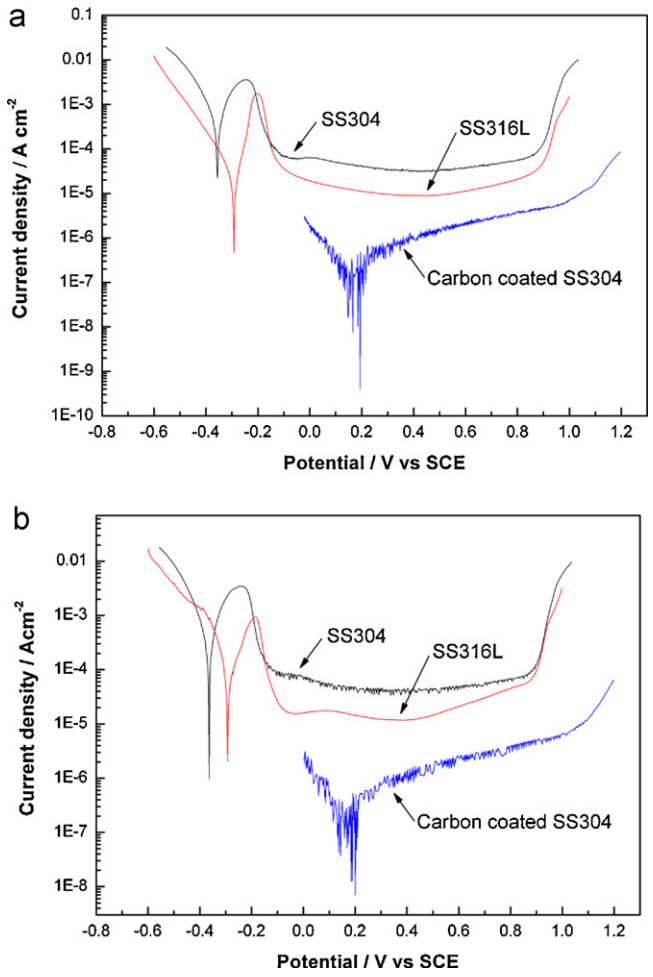

Fig. 5. Potentiodynamic curves of the bare SS304 and SS316L and the carbon-coated SS304 in 0.5 M H_2SO_4 + 2 ppm F^- solution at 80 °C: (a) bubbled with air and (b) bubbled with hydrogen.

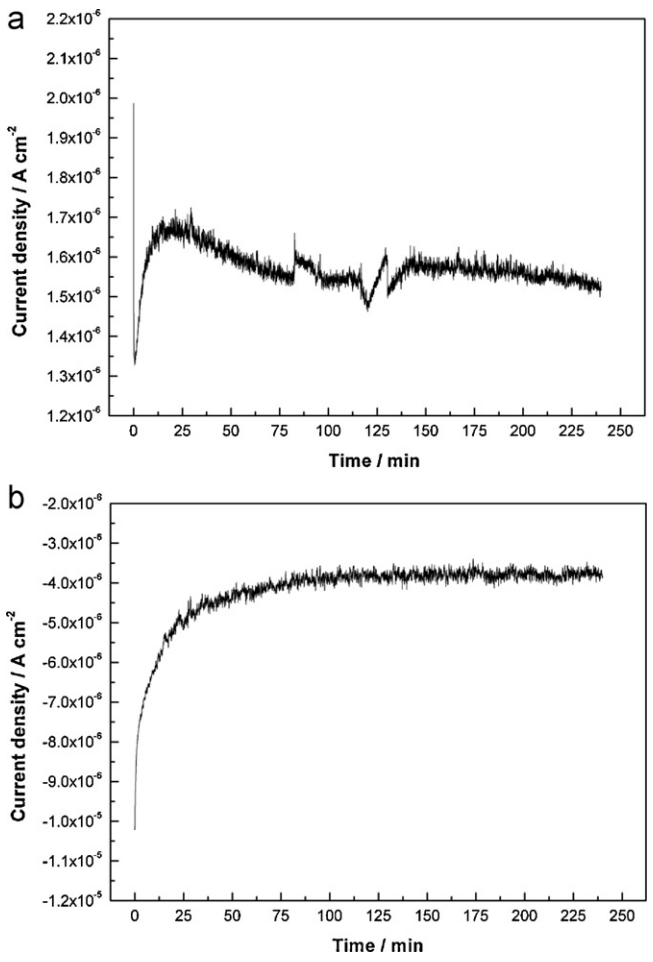

Fig. 6. Potentiostatic curves of the carbon-coated SS304 in the (a) simulated cathode (0.6 V bubbled with air) and (b) anode (−0.1 V bubbled with hydrogen) environments.

According to the above potentiodynamic results, it can be concluded that the passive current density of the uncoated SS304 and SS316L are still very high and the passive film formed on their surfaces cannot resist corrosion due to their weak resistance to the simulated PEMFC environment, although both of them have obvious passive regions in the simulated cathode and anode environments that are beneficial to protecting themselves against corrosion in the simulated environment. In contrast to the bare SS304 and SS316L, the carbon coated SS304 has a significant decrease in the corrosion current density in the simulated cathode and anode environments, which indicates that the corrosion resistance of the carbon-coated SS304 is greatly improved. This improvement is the result of the CUBMSIP process in which there is high ion current density surrounding the substrates and intense ion bombardment on the growing film, which contribute to the deposition of very dense film with few defects. This dense carbon film on SS304 is beneficial because it prevents the corrosion solution from penetrating to the substrate to protect the substrate against the simulated PEMFC environment.

To investigate the stability of the carbon film at the cathodic and anodic operation potentials in the simulated PEMFC environment, potentiostatic tests were performed for 4 h. The potentiostatic curves of the carbon-coated SS304 are shown in Fig. 6. The transient current density at the cathodic operation potential decays quickly at the beginning, then increases slightly and eventually maintains a stable low value of approximately 1.56 μA cm^{-2}, which is helpful for substrate protection. The value of the corrosion current density at the anodic operation potential is negative throughout the test process, and the final stable corrosion current density reaches a relatively low level. This test demonstrates that the carbon film operates in the cathodic state and can protect the substrate in the simulated anode environment. Therefore, the potentiostatic polarisation result indicates that the carbon film is stable in both the simulated cathode and anode environments and provides good protection to the substrate, which is in agreement with the result of the potential dynamic polarisation.

Fig. 7 shows SEM images of a surface micrograph of the carbon-coated SS304 after the potentiostatic tests in the simulated cathode and anode environments. There are only a few white substances on the film surface, and no overall and local corrosion occurs. This result is likely related to the dense high-performance carbon film on the SS304. Therefore, the carbon-coated SS304 exhibits excellent corrosion resistance in the simulated cathode and anode PEMFC environments.

3.3. Interfacial contact resistance

The interfacial contact resistance of the bare and carbon-coated SS304 are shown in Fig. 8. In the deposition process of the translation layer, the chromium target current and the graphite target current change continuously; thus, the stoichiometric ratio of transition layer is graded. The resistivity of the transition layer is not expected to be as high as that of the chromium carbide with a con-

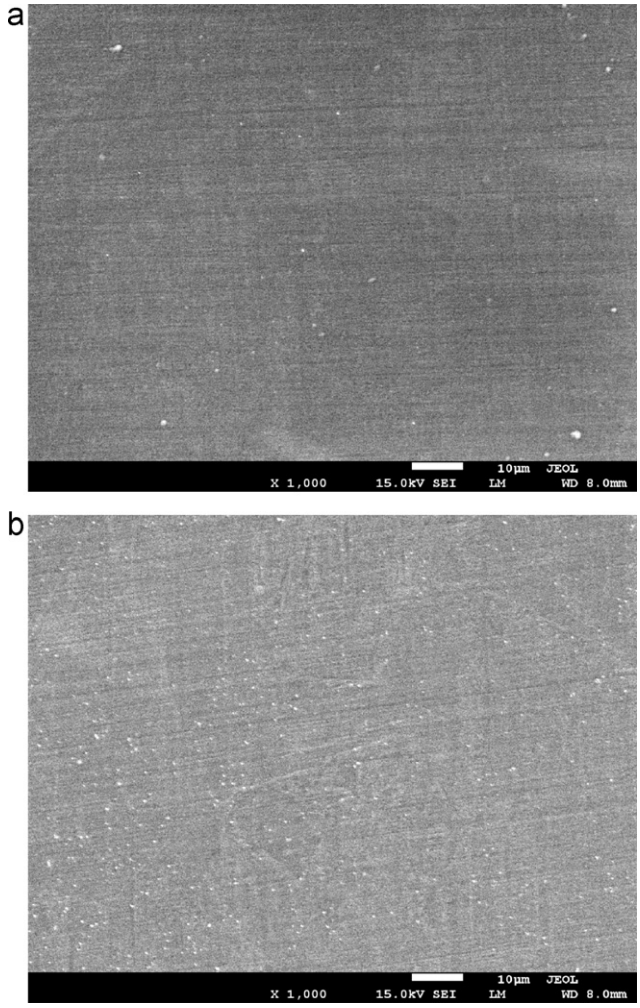

Fig. 7. SEM images of the surface micrograph of the carbon-coated SS304 after the potentiostatic test in the (a) cathode environment and (b) anode environment.

stant stoichiometric ratio. Therefore, the measured value of ICR can represent the ICR between the carbon film and the conductive carbon paper. From Fig. 8, it can be seen that the ICR decreases quickly under low compaction force because the contact points between the testing sample and the carbon paper increase as the compaction

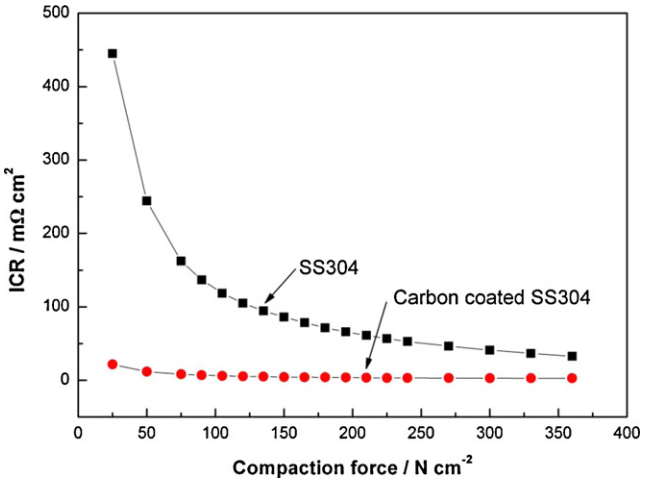

Fig. 8. Interfacial contact resistance of the bare and carbon-coated SS304 with carbon paper.

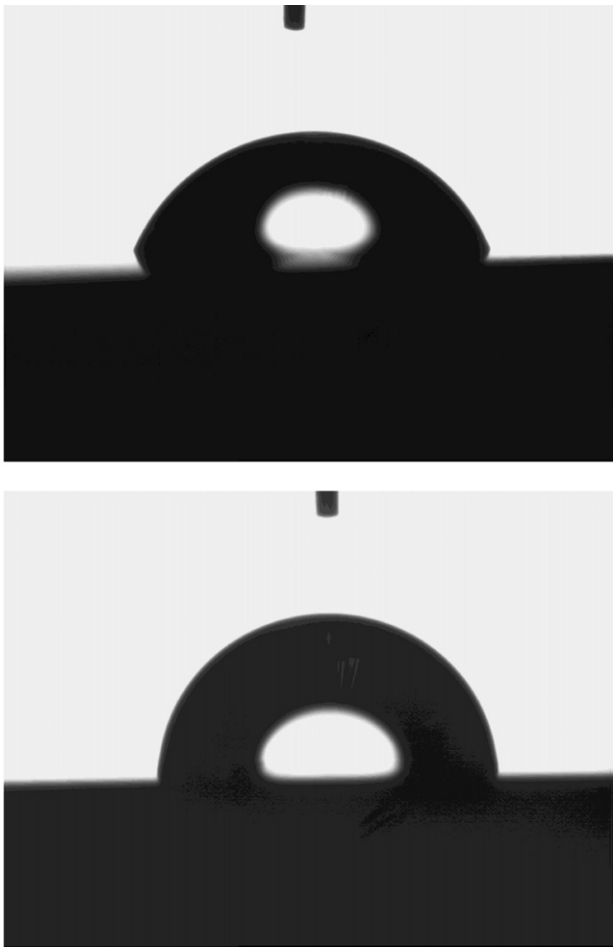

Fig. 9. Contact angle images of the uncoated and carbon-coated SS304 with water.

force increases, and the ICR is mainly influenced by a low compaction force. Then, the ICR gradually decreases and finally remains steady because the contact area between the carbon-coated SS304 and the carbon paper gradually reaches the maximum, and the compact force is no longer the main influence on the ICR.

Fig. 8 also shows that the ICR between the SS304 and the carbon paper is very high because of the weak conductivity of the passive film formed on the surface. Compared to SS304, the carbon-coated SS304 has a much lower ICR. The ICR between the carbon-coated SS304 and the carbon paper is 8.28–2.59 $m\Omega\,cm^2$ under compaction forces between 75 and 360 $N\,cm^{-2}$. The ICR of carbon-coated SS304 decreases from 94.44 $m\Omega\,cm^2$ to 4.92 $m\Omega\,cm^2$ at 135 $N\,cm^{-2}$. The low ICR between the carbon-coated SS304 and the carbon paper is a result of the high conductivity of the carbon film. Low ICR is an important factor that influences the output power of the fuel cell stack and can increase the durability of the fuel cell stack, which may lead to its industrialisation.

3.4. Contact angle

Fig. 9 shows the contact angle images of the uncoated and carbon-coated SS304 with water. Fig. 10 shows the contact angle value of the bare and carbon-coated SS304 with water. To achieve an accurate value, four measurements are collected for each specimen. The average contact angle value of the SS304 is 67.4°, while the carbon-coated SS304 has a much larger average contact angle: 88.6°. Water is produced during the operation of the PEMFC. If the generation rate of liquid water at the cathode exceeds the removal rate from the cathode, the water will flood. Water flooding can hin-

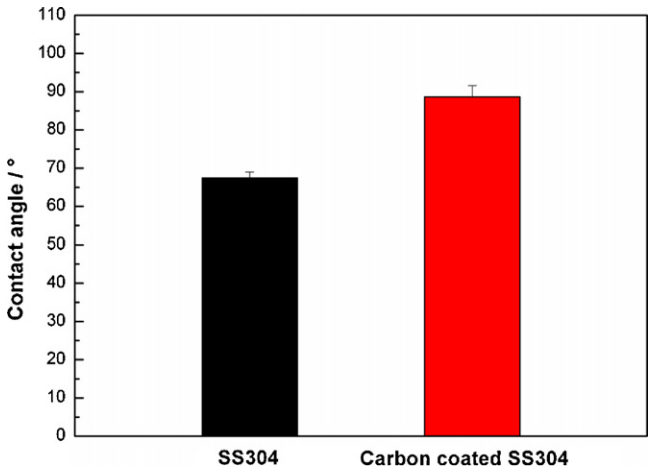

Fig. 10. Contact angle value of the uncoated and carbon-coated SS304 with water.

der oxygen transport and blocks the surface area of the catalysts, which will lead to a significant decrease in fuel cell performance. Therefore, water should be removed successfully, and the bipolar plate should be hydrophobic. The contact angle increases with improvement in the hydrophobic property, which contributes to water removal in the fuel cell stack. The large contact angle of the carbon-coated SS304 with water favours water removal to prevent accumulated water from flooding the electrode system.

4. Conclusions

Carbon film has been sputtered on the SS304 by close field unbalanced magnetron sputter ion plating for use as bipolar plates for PEMFC. This carbon-coated SS304 exhibits good corrosion resistance, high conductivity and high hydrophobicity; therefore, it has great potential for application as bipolar plates for the fuel cell stack. The corrosion current density of the carbon-coated SS304 decreases to 2.10 $\mu A\,cm^{-2}$ at 0.6 V in the simulated cathode environment, which is one order of magnitude lower than that of the SS304. The open circuit potential of the carbon-coated SS304 increases to 206 mV and 214 mV in the simulated cathode and anode environments, respectively, which are far higher than that of the SS304. The interfacial contact resistance between the carbon-coated SS304 and the carbon paper reaches a very low value of 4.92 $m\Omega\,cm^2$ under a compaction force of 135 $N\,cm^{-2}$. The contact angle between the carbon coated SS304 and water (67.4°) is lower than that between the uncoated SS304 and water (88.6°).

Acknowledgements

This work is financially supported by the National Natural Science Foundation of China (Grant No. 50971091 and Grant No. 50820125506), and the Ministry of Science and Technology of the People's Republic of China (Grant No. 2009DFB50350).

References

[1] B.C.H. Steele, A. Heinzel, Nature 414 (2001) 345–352.
[2] H. Tsuchiya, O. Kobayashi, Int. J. Hydrogen Energy 29 (2004) 985–990.
[3] X.G. Li, I. Sabir, Int. J. Hydrogen Energy 30 (2005) 359–371.
[4] H. Tawfik, Y. Hung, D. Mahajan, J. Power Sources 163 (2007) 755–767.
[5] V. Mehta, J.S. Cooper, J. Power Sources 114 (2003) 32–53.
[6] J. Wind, R. Spah, W. Kaiser, G. Bohm, J. Power Sources 105 (2002) 256–260.
[7] T. Kinumoto, M. Inaba, Y. Nakayama, K. Ogata, R. Umebayashi, A. Tasaka, Y. Iriyama, T. Abe, Z. Ogumi, J. Power Sources 158 (2006) 1222–1228.
[8] R.C. Makkus, A.H.H. Janssen, F.A.D. Bruijn, R.K.A.M. Mallant, J. Power Sources 86 (2000) 274–282.
[9] D.P. Davies, P.L. Adcock, M. Turpin, S.J. Rowen, J. Power Sources 86 (2000) 237–242.
[10] N. Sammes, Fuel Cell Technology: Reaching Towards Commercialization, Engineering Materials and Processes, Germany, 2006, pp. 27–51.
[11] M.P. Brady, K. Weisbrod, I. Paulauskas, R.A. Buchanan, K.L. More, H. Wang, M. Wilson, F. Garzon, L.R. Walker, Scr. Mater. 50 (2004) 1017–1022.
[12] Y. Wang, D.O. Northwood, Int. J. Hydrogen Energy 32 (2007) 895–902.
[13] Y. Fu, M. Hou, G. Lin, J. Hou, Z. Shao, B. Yi, J. Power Sources 176 (2008) 282–286.
[14] D.G. Teer, US Patent 5,556,519 (1996).
[15] T. Fukutsuka, T. Yamaguchi, S.I. Miyanoa, Y. Matsuo, Y. Sugi, Z. Ogumib, J. Power Sources 174 (2007) 199–205.
[16] Y. Show, Surf. Coat. Technol. 202 (2007) 1252–1255.
[17] Y. Fu, M. Hou, G. Lin, J. Hou, Z. Shao, B. Yi, Int. J. Hydrogen Energy 34 (2009) 405–409.
[18] M. Li, S. Luo, C. Zeng, J. Shen, H. Lin, C. Cao, Corros. Sci. 46 (2004) 1369–1380.
[19] R. Tian, J. Sun, L. Wang, Int. J. Hydrogen Energy 31 (2006) 1874–1878.
[20] E.A. Cho, U.S. Jeon, S.A. Hong, I.H. Oh, S.G. Kang, J. Power Sources 142 (2005) 177–183.
[21] K. Feng, X. Cai, H. Sun, Z. Li, P.K. Chu, Diamond Relat. Mater. 19 (2010) 1354–1361.
[22] K. Feng, Y. Shen, H. Sun, D. Liu, Q. An, X. Cai, P.K. Chu, Int. J. Hydrogen Energy 34 (2009) 6771–6777.
[23] J. Zhang, Vacuum 5 (1992) 23–28.
[24] Y. Wang, D.O. Northwood, Electrochim. Acta 52 (2007) 6793–6798.
[25] H.S. Choi, D.H. Han, W.H. Hong, J.J. Lee, J. Power Sources 189 (2009) 966–971.
[26] H. Wang, M.A. Sweikart, J.A. Turner, J. Power Sources 115 (2003) 243–257.